



Published in final edited form as:

Hypertension. 2015 July ; 66(1): 199–210. doi:10.1161/HYPERTENSIONAHA.115.05610.

BNP DELETION LEADS TO PROGRESSIVE HYPERTENSION, ASSOCIATED ORGAN DAMAGE, AND REDUCED SURVIVAL: A NOVEL MODEL FOR HUMAN HYPERTENSION

Sara J. Holditch¹, Claire A. Schreiber¹, Ryan Nini¹, Jason M. Tonne¹, Kah-Whye Peng¹, Aron Geurts², Howard J. Jacob², John C. Burnett³, Alessandro Cataliotti^{3,4}, and Yasuhiro Ikeda¹

¹Department of Molecular Medicine, Mayo Clinic, College of Medicine, Rochester, MN, USA

²Department of Physiology, Cardiovascular Center, Medical College of Wisconsin, Milwaukee, WI, USA

³Cardiorenal Research Laboratory, Division of Cardiovascular Diseases, Departments of Medicine and Physiology, Mayo Clinic, College of Medicine Rochester, MN, USA

⁴Institute for Experimental Medical Research, Oslo University Hospital, University of Oslo, Oslo, Norway

Abstract

Altered myocardial structure and function, secondary to chronically elevated blood pressure, are leading causes of heart failure and death. B-type natriuretic peptide, a guanylyl cyclase A agonist, is a cardiac hormone integral to cardiovascular regulation. Studies have demonstrated a causal relationship between reduced production and/or impaired B-type natriuretic peptide release, and the development of human hypertension. However, the consequences of B-type natriuretic peptide insufficiency on blood pressure and hypertension-associated complications remain poorly understood. Therefore, the goal of the current study was to create and characterize a novel model of B-type natriuretic peptide deficiency to investigate the effects of B-type natriuretic peptide absence on cardiac and renal structure, function, and survival.

Genetic B-type natriuretic peptide deletion was generated in Dahl Salt Sensitive rats. Compared to age-matched controls, B-type natriuretic peptide-knockout rats demonstrated adult-onset hypertension. Increased left ventricular mass with hypertrophy and substantially augmented hypertrophy signaling pathway genes, developed in young adult knock-out rats, which preceded hypertension. Prolonged hypertension led to increased cardiac stiffness, cardiac fibrosis, and thrombi formation. Significant elongation of the QT interval was detected at nine months in knock out rats. Progressive nephropathy was also noted with proteinuria, fibrosis, and glomerular alterations in B-type natriuretic peptide knock out rats. End organ damage contributed to a significant decline in overall survival. Systemic B-type natriuretic peptide over-expression reversed the phenotype of genetic B-type natriuretic peptide deletion.

Corresponding author: Yasuhiro Ikeda, PhD Department of Molecular Medicine Mayo Clinic, 200 First St. SW, Rochester MN 55905, USA **Fax:** 507-266-2111, **Phone:** 507-538-0153 Ikeda.yasuhiro@mayo.edu.

Conflicts of Interest / Disclosures: None.

Our results demonstrate the critical role of B-type natriuretic peptide defect in the development of systemic hypertension and associated end organ damage in adulthood.

Keywords

Natriuretic peptide; hypertrophy; fibrosis; hypertension; kidney; cardiac function

INTRODUCTION

Hypertension is associated with considerable morbidity and mortality, presenting a major public health concern. If untreated, chronic cardiac overload results in hypertensive heart disease, characterized by cardiac remodeling, fibrosis, and stiffness, ultimately leading to heart failure¹. Chronic hypertension can also cause nephropathy, associated with renal fibrosis and glomerular pathologies. Chronic hypertension alone is a major risk factor for stroke and arterial disease².

Accepted as an important endocrine organ³, the heart is involved in the regulation of pressure and volume by secreting hormones; atrial-natriuretic peptide (ANP) and B-type natriuretic peptide (BNP)^{3,4}. These peptides are produced in response to excessive cardiomyocyte stretching⁵ and maintain cardiovascular integrity through binding guanylyl-cyclase A (GC-A) (also known as natriuretic peptide receptor 1, Npr1)⁶. Acting as paracrine and autocrine factors, ANP and BNP show direct antifibrotic and antihypertrophic effects⁷. Both clinical and animal studies have established the importance of ANP and BNP in cardiorenal homeostasis. In the clinic, circulating levels of BNP has become a well-recognized biomarker with diagnostic and prognostic implications in heart failure patients, as well as in chronic kidney disease progression⁸. Additionally, human recombinant BNP, nesiritide, is available for the treatment of dyspnea in patients with acute heart failure, while studies are ongoing to explore its potential clinical use in resistant hypertension. In this regard, a small clinical study has shown, in uncontrolled hypertension, normalization of blood pressure (BP) following subcutaneous nesiritide without the need for further antihypertensive medications⁹.

Likewise, transgenic mouse studies looking at BNP overexpression show significantly reduced BP, and protection from cardio-renal remodeling from a variety of assaults¹⁰⁻¹². Similarly, vector-mediated cardiac over-expression of BNP prohormone (proBNP) prevents BP elevation and the development of hypertensive heart disease in spontaneously hypertensive rats and significantly improved survival in rats with overt hypertensive heart disease^{13,14}. Consistent with these animal studies, variations in the coding regions of ANP and BNP have been causally linked to increased circulating ANP or BNP levels in humans, which in turn are associated with lower BP and a reduced risk of clinical hypertension¹⁵.

Conversely, suboptimal BNP production or release has been implicated as a contributor in the development of human hypertension¹⁶. Analysis of population-based samples, known as the PAVD (Prevalence of Asymptomatic Ventricular Dysfunction) cohort (N=2,082, age >45 years), has shown impaired production and/or release of proBNP(1-108) with

simultaneous reduction of circulating BNP(1-32) and NT-proBNP(1-76) and ANP in subjects with the early stages of hypertension^{17, 18}.

Better defining the deleterious effects of BNP insufficiency, mouse models with genetic deletions in ANP or GC-A are characterized by marked congenital left ventricular hypertrophy (LVH) and systemic hypertension⁷. Importantly, the mouse model of systemic BNP gene (*Nppb*) disruption exhibits focal cardiac fibrosis upon pressure-overload, however it lacks evidence of elevated BP, and LVH^{19, 20}, two hallmarks of human hypertension. Along with the absence of secondary sequelae inherent to hypertension, such as the cardiorenal interplay, the knock out mouse model poorly reflects clinical outcomes – such as progressive and chronic organ remodeling and loss of function.

Clinical biomarker studies, pharmaceutical supplemental-BNP advances, and knock out model observations, cumulatively, fall short of a systematic approach in explaining the role of BNP insufficiency on the development of hypertension and hypertension-associated complications. To elucidate the functional significance of BNP on the progression of hypertension and associated sequelae, we characterized genetically BNP-null (*Nppb*^{-/-}) rat lines. We observed progressive hypertension, cardiac remodeling, decreased myocardial function, aggravated renal pathologies, and an aggressive decline in overall survival compared to age-matched controls. This study provides a model for furthering our understanding of hypertension associated with a deficiency of the BNP system and the sequelae that arise.

METHODS

All animal procedures were approved by Mayo Clinic Institutional animal care and use committee.

Animals

Nppb^{-/-} rats were generated on Dahl Salt Sensitive (Dss) backgrounds as described previously²¹. Further details, including hematology and urinalysis, tissue harvesting, and rna extraction, are included in the Online Data Supplement.

BP measurement

Noninvasive blood pressure is measured by tail-cuff using the CODA high throughput non-invasive BP system (Kent Scientific), detailed previously^{6, 13}. Invasive blood pressure measurements, including surgical procedures as detailed by StellarTelemetry, are included in the Online Data Supplement.

Histology

For light microscopy, organs were sectioned (7-12 μm thick) from OTC-embedded specimens and stained with hematoxylin and eosin or Masson's trichrome staining. Cardiac fibrosis areas were imaged by a light microscope (Axioplan). Trichrome stained tissues were analyzed by KS400 Image Analysis Software (version 3.0, Zeiss).

Confocal microscopy

Kidney architecture in wild-type, and *Nppb*^{-/-} rats were analyzed by immunofluorescence using antibodies against desmin (Anti-desmin Antibody, clone DEB-5, Millipore), EPCAM-1 (Anti-EPCAM-1 antibody ab71916, Abcam), and podocin (rabbit anti-podocin antibody, Sigma), fibroblast growth factor 2 (FGF-2 antibody (G-2) sc-365106, Santa Cruz Biotechnology, Santa Cruz, CA), aquaporin 2 (AQP2 (C-17), sc-9882, Santa Cruz Biotechnology, Santa Cruz, CA) and with the nuclear probe 4', 6-diamidino-2-phenylindole-2HCl (Invitrogen). Fluorescent images were obtained with a Laser Scanning Microscope 510 (Zeiss, Thornwood, NY) and analyzed using Zeiss Laser Scanning Microscope Image Browser.

OTC-embedded kidney tissue sections were cryosectioned to 12 μ m thickness, mounted on frosted slides, and air dried. Before the incubation with specific antibodies, sections were fixed in acetone at -20°C for 20 minutes, air dried, and washed in PBS. To prevent nonspecific binding of immunoglobulins (IgGs), tissues were blocked for 1h (PBS/1% fetal bovine serum). Sections were incubated with primary antibodies diluted 1:300 in blocking solution overnight at 4°C . Day 2, samples were washed 3 times (10 minutes each) with PBS and incubated with secondary antibodies at 1:1000 in blocking solution (Alexa Fluor 568 donkey anti-mouse, Alexa Fluor 594 donkey anti-goat, Alexa Fluor 647 donkey anti-rabbit IgG) for 1h at room temperature. Next, tissues were washed 3 times (5 minutes each) with PBS, and then incubated with DAPI (1:3000) for 5 minutes at room temperature. Afterwards, slides were washed with PBS and then mounted with Dako Fluoro Mounting Media (Dako, Carpinteria, CA).

Echocardiography (ECHO) for non-invasive assessment of cardiac function and structure

Standard ECHO examinations were performed at 3, 6 and 9 months in *Nppb*^{-/-} and control rats. All ECHO examinations, ECHO analysis, and speckle tracking were performed by a skilled sonographer (S.H) blinded to treatment, as previously described^{13, 14}. Further details are included in the online data supplement.

Statistical analysis

Comparisons between groups were made with unpaired Student's t-tests. Comparisons of BP values between groups were performed by two-way ANOVA, and Sidak's multiple comparison test for repeated measurements. Survival curves were compared by log-rank (Mantel-Cox) test. Data are expressed as mean \pm standard deviation. Significance was predetermined as $p < 0.05$ and n refers to sample size.

RESULTS

BNP knockout rats demonstrate progressive BP elevation

Two *Nppb*^{-/-} lines were generated as previously described^{21, 22}. *Nppb*^{-/-} M2 and M4 lines have deletions of 100 bp and 138 bp bracketing intron 1 and exon 2 (Fig. 1A). Figure 1B represents the genotyping results of wildtype, *Nppb*^{-/-} M2, and *Nppb*^{-/-} M4 rats upon PCR amplification of the *Nppb* intron 1 and exon 2 junction. Since M2 and M4 rat strains developed fundamentally identical cardiorenal phenotypes, here, we report the results of

Nppb^{-/-} M2 rats. When compared to age-matched rats, BNP-knockout rats demonstrated trends of elevated BP beginning at four months of age, with chronically elevated diastolic, mean, and systolic BP at six months (Fig. 1C). To verify the BP measurements, we implanted telemetry devices into the descending aorta and measured BP in conscious rats at three, six, and nine months of age (Fig. 1D). Telemetry results confirmed significantly elevated BP in aged Nppb^{-/-}, consistent with the tail-cuff data set (Fig. 1C),

Genetic BNP deletion leads to development of LV hypertrophy in young adults, with increased cardiac stiffness and fibrosis and QT elongation

ECHO parameters—ECHO results are summarized in Table 1. ECHO analysis at one and two months of age revealed no notable difference in cardiac parameters between Nppb^{+/+} and Nppb^{-/-} rats. At three-months, however, genetic BNP-null rats exhibited significant LV hypertrophy (LVH), augmented interventricular septum (IVS) and left ventricular posterior wall (LVPW) thickness, with no change in LV chamber dimensions compared to age-matched controls. At this time, Nppb^{-/-} rats experienced a concentric pattern of LVH, with maintained LV function compared to Nppb^{+/+}. At six months, Nppb^{-/-} rats maintained hypertrophied LV mass when compared to Nppb^{+/+}, with transitions into dilated cardiomyopathy, as indicated by augmented internal chamber diameters. At nine-months of age, surviving Nppb^{-/-} rats develop dilated LV chambers, along with narrower LVPW thickness, with comparable ejection fraction and percent fractional shortening between groups.

To better characterize the cardiac phenotype, we further examined 2D ECHO images with Speckle-tracking to assess myocardial strain at three and nine months (Table 2), revealing a significant reduction in both radial strain, as well as radial strain rates during early (at three and nine months) and late diastole (at nine months) in Nppb^{-/-}.

Cardiac phenotype—We then characterized the structure of cardiac tissues at three and nine months. At three months of age, collagen deposition in cardiac sections between Nppb^{+/+} and Nppb^{-/-} were similar, as assessed by Masson's trichrome staining. However, at nine months, Nppb^{-/-} exhibited enhanced collagen deposition throughout the myocardium, altered structure and organized LV thrombi compared to Nppb^{+/+} (Fig. 2A). Additionally, we observed approximately one in four Nppb^{-/-} exhibiting an abnormal cardiac structure with localized fibrosis at three and nine months, and organized LV thrombi at three months of age. These phenotypes (fibrosis and thrombi formation) were absent in age-matched rats, as shown in Figure 2A, with knock out thrombi illustrated in (Fig. 2B). Quantitative RT-PCR identified significantly elevated expression of canonical fibrosis-associated genes at three months, including tissue inhibitor of metalloproteinase 1 (Timp1), fibronectin-1 (Fn1), transforming growth factor-beta (Tgfb), collagen type 1 alpha 1 (Col1a1), and vascular endothelial growth factor (Vegf) (Fig. 2C). Of note, these transcripts were up-regulated at three months, prior to significant LVH, as well as deposition of connective tissues in the heart of Nppb^{-/-} (Fig. 2A, Right). Additionally, telemetry data collected at three, six, and nine months, revealed significantly elongated QT duration in Nppb^{-/-} rats at nine months (Fig 2D). Heart rate variability (HRV) was similar at early, three months, and later, nine

months, time points between knock out and control rats (Fig 2D), though cardiac expression of nerve growth factor (Ngf) was slightly depressed in the knockout rat.

Survival Analysis and Necropsy—*Nppb*^{-/-} rats showed a significant decline in the survival, mainly observed as sudden death (Fig. 2F). Necropsy was performed on as many of the animals as possible within 24 hrs of death or euthanasia. Of eight adult *Nppb*^{-/-} rats, none presented with pathological changes typical of congestive heart failure. Two presented with pericardial hemorrhage. Two animals showed sudden onset of lethargy with stroke-like balance problems, although no evidence of death from cerebral hemorrhage or ischemia was observed. All aged BNP-null rats showed darkened, stiff kidneys with rough surfaces, with blood tests indicating impaired, but functioning kidneys.

Up-regulation of hypertrophic signaling pathways, cardiac contractility genes, and calcium influx in the *Nppb*^{-/-} rat hearts

To better interrogate the primary networks affected by genetic BNP deletion at a prehypertensive state (three months of age), we carried out genome-wide expression profiling of LV tissues. Initial transcriptome analysis identified strongly down-regulated genes in the *Nppb*^{-/-} rat, including key factors in cardiac repair/regeneration/angiogenesis (*Sdf1/Cxcl12*, *Nrp1*, *Dll4*, *Notch1*), actin-regulating/binding factors (*Ablim1*, *Tmod2* and *Wasf2*), and factors associated with activation of cyclic AMP pathway (*Gpr4*, *Adcy4*) or coagulation (*F5*) (Fig. 3A). Highly activated genes in BNP ablation included a cardiac stretch sensor *Lrrc39*²³, factors critical in contractility (cardiac alpha actin/*Actc1* and *Tropomyosin1/Tpm1*), MAP kinase kinase kinase family protein *Tnni3k*, transthyretin (*Ttr*), factors involved in glycolysis (*Pfkm*) or lipid droplet accumulation (*Fitm1*), and adenosine kinase (*Adk*), responsible for phosphorylating adenosine, a cardioprotective agent (Fig. 3A). Further bioinformatic network analysis identified the strongest toxicity responses up-regulated in *Nppb*^{-/-} were hypertrophy signaling, cardiac necrosis/cell death, and cardiac fibrosis (Fig. 3B, Supplemental Figure S1, S2 and S3). Importantly, familial hypertrophic cardiomyopathy genes were potentially up-regulated in *Nppb*^{-/-} hearts (Fig. 3C). Further analysis of key cardiac genes, responsible for cardiac contractility and relaxation, demonstrated clear trends in enhanced contractility and increased Ca²⁺ influx upon BNP ablation (Fig. 3D, Supplemental Figure. S4).

We confirmed the microarray data by quantitative RT-PCR, and observed augmented *Ttr* expression, significantly elevated *Actc1*, myosin heavy chain 7 (*Myh7*), and *Tpm1* expression in *Nppb*^{-/-} hearts at three months, compared to controls (Fig. 3E). Likely due to cardio-compensation, we observed elevated levels of ANP- and C-type natriuretic peptide (CNP) transcripts (*Nppa*, *Nppc*), as well as NP receptors, *Npr1*, 2, and 3 in *Nppb*^{-/-}. Although *Nppb* transcripts no longer encode intact BNP, RT-PCR amplifying the non-coding *Nppb* exon 1 region also showed increased levels in *Nppb*^{-/-} rats. No significant difference was observed in control 18s ribosomal RNA transcript levels between *Nppb*^{-/-} and *Nppb*^{+/+} animals.

Development of hypertensive nephropathy

Renal function and pathology was assessed. Blood and urinalysis at study termination (nine months) revealed increased urine excretion and proteinuria in *Nppb*^{-/-}, although no difference was observed in creatinine clearance between controls and survived knockout rats (Fig. 4A). Histologically, renal sections of *Nppb*^{-/-} rats at three and nine months displayed progressive glomerular alterations, characterized by a marked thickening of the glomerular basement membrane and glomerular sclerosis (Fig. 4B and 4C). Desmin, podocin and EPCAM-1, were characterized through immunofluorescence of renal sections at three and nine months. Increased desmin and decreased podocin staining was observed with age in both *Nppb*^{-/-} and *Nppb*^{+/+} rats (Fig. 4D), though more prominent in *Nppb*^{-/-} rats. No notable difference was observed in anti-EPCAM-1 antibody staining (Fig. 4D).

Nppb^{-/-} renal tissues at nine months exhibited micro-cysts, prominent renal casts and interstitial fibrosis (Fig. 4E, left panel). Staining with lotus tetragonolobus agglutinin (LTA), a marker of proximal tubules, and aquaporin 2 (AQP2), a collecting duct marker, identified micro-cysts were predominantly LTA-positive (Fig. 4E, middle and right panel). Renal tissues in prehypertensive *Nppb*^{-/-} rats exhibited up-regulation of fibrosis genes, such as *Tgfb* and *Col1a1*, as well as up-regulation of natriuretic peptide pathway genes, such as *Npr1* and *Npr2*, at three months of age, as assessed by qRT-PCR (Fig. 4F).

Activation of renal toxicity response pathways in the early phase of hypertension

To better interrogate the primary networks affected by BNP knock out at a prehypertensive state (three months of age), we carried out genome-wide expression profiling of renal tissues. Bioinformatic network analysis identified the strongest toxicity responses up-regulated in *Nppb*^{-/-} were renal, renal necrosis / cell death, renal tubule injury, renal hydronephrosis, and kidney failure (Fig. 4G and Supplemental Figure S6A). Analysis of the most differentially suppressed genes identified BMP signaling (*Fst* and *Mras*), LPS and IL-1 mediated inhibition of RXR function (*Acox2*) and Protein Kinase A Signaling (*Ppp1r1b*, *Ptpro*) in knock out tissues. The most differentially augmented pathways were the Acute Phase Response Signaling (*apcs*), Calcium signaling (*tnnc1*), Coagulation system (*Serpinc1*), Prostanoid Biosynthesis (*Ptgds*), and IL-12 Signaling and Production in Macrophage pathway (*ApoE*). Most, being pathways involved in inflammatory responses providing protection from assault with non-specific defense mechanisms, or pathways involved in ischemia responses^{24, 25}(Supplemental Figure S6B). We confirmed the microarray data by quantitative RT-PCR, and observed significantly elevated *Slc4a4*, *G6pc*, *Nphs1*, and *ApoE1* expression in *Nppb*^{-/-} kidneys at three months, compared to controls (Supplemental Figure S6C).

Salt-sensitive BP elevation in BNP knockout rats

Our *Nppb*^{-/-} rat was derived from a *Dss* rat, which presents with a nearly normal cardiovascular and renal phenotype if not conditioned with increased sodium diet. To see the influence of BNP knock out on salt-induced hypertension, we fed 10-week-old *Nppb*^{+/+} *Dss* and *Nppb*^{-/-} *Dss* rats a high salt diet for 3 weeks, and monitored BP. When compared to age-matched controls, *Nppb*^{-/-} rats demonstrated slightly elevated BP prior to the high salt diet. Three weeks of high sodium diet induced similar degrees of BP elevation in both *Nppb*

–/– and *Nppb*^{+/+} Dss (Fig. 5A). Echo baseline measurements were not taken; presenting a valid limitation as to the interpretation of myocardial changes diet could induce in three weeks. However, comparisons between age-matched knock out and control rats 3 weeks post high-salt diet showed salt-induced hypertension with significantly wider IVS, a narrowing of the LV diameter, and a thicker LVPW in *Nppb*^{–/–} rats compared to controls (Fig. 5B). Urinary parameters analyzed showed trends of worsened proteinuria, and lower creatinine clearance, in *Nppb*^{–/–} rats compared to *Nppb*^{+/+} rats after high sodium diet (Fig. 5C).

DISCUSSION

The current study demonstrates that BNP deletion, in a novel rat knockout model, is characterized by progressive and sustained increase in BP. Interestingly, elevation of BP was preceded by early myocardial alteration as detected by echo assessments, immunostaining studies and gene expression analysis. Chronic hypertension was also associated with progressive structural and functional alterations of the kidneys, and reduced survival.

BNP defect leads to adult-onset systemic BP elevation

The healthy heart responds to cardiac overload by releasing ANP and BNP into the circulation. Once disseminated, natriuretic peptides (NPs) induce vasodilation and stimulate renal natriuresis through binding receptor GC-A/Npr1^{26, 27}. Although ANP and BNP are functioning largely in a similar fashion, BNP has unique anti remodeling properties, greater stability, and rapid gene induction in response to cardiac stress²⁷⁻³¹. A large association study has linked single nucleotide polymorphisms (SNPs) in the *Nppb* and *Nppa* locus (rs5068, rs198358 or rs632793) to increased circulating NP levels, and congruently lower systolic and diastolic BP, as well as a reduction in the risk of developing hypertension³². Conversely, a study on the relationships between levels of BNP and the severity of hypertension in subjects with mild, moderate, and severe hypertension has revealed that there are reduced levels of processed forms of BNP, namely NT-proBNP1-76 and BNP1-32, in the early phase of hypertension¹⁶. Our recent population study developed upon this observation, by showing a relative deficiency of the circulating BNP precursor proBNP1-108 in prehypertensive, and early stage hypertensive subjects¹⁸. This indicates that suboptimal circulating levels of BNP play a vital role in the development of adult-onset human hypertension. Here, we have demonstrated significant and chronically elevated BP in young adult rats with genetic BNP deletion. In agreement with a large body of literature^{33, 34} we previously reported¹⁴ that non-invasive (tail-cuff, CODA) BP measurements are inflated, though consistent and correlated to invasive-telemetric BP measurements. *Nppb*^{–/–} rats experienced elevated BP when assessed by either non-invasive tail-cuff or by telemetry (e.g. telemetry SBP from 127 at three months to 210 mmHg at nine months in the *Nppb*^{–/–} rats vs 127 at three months and 123 mmHg and nine months in the *Nppb*^{+/+} rats), verifying the link between BNP insufficiency and increased BP. Progressive hypertension in the *Nppb*^{–/–} rats on low salt diet is consistent with the reported phenotype of the GC-A/Npr1 knockout mice on a 129/B6 hybrid background³⁵. Intriguingly, the mouse model of genetic BNP ablation on a pure 129/Sv background is characterized by multifocal fibrosis devoid of

systemic hypertension²⁰. One assumption is the difference in compensatory ANP responses, i.e., intact and defective ANP responses in 129/Sv and Dss rats, respectively. However, Dss rats have intact ANP responses capable of counteracting BP elevation and salt-induced hypertension³⁶. We also confirmed activation of ANP, and CNP expression in BNP-deficient rats (Fig. 3F) that may provide a possible explanation for the lack of cardiac hypertrophy despite the increase in BP in *Nppb*^{-/-} rats. Indeed, reports suggest that cardiac-derived CNP becomes more important in preserving heart structure and function with time in mice with left ventricular hypertrophy and heart³⁷.

Based on our findings, we speculated that the role of BNP in controlling BP goes, at least in part, beyond sodium regulation. In fact, the similar degree of increase in BP, observed in both the *Nppb*^{-/-} and the control rats fed with high salt diet for three weeks, suggested that the mechanisms of BP elevation are independent of sodium homeostasis and mutually exclusive. It is possible that other prohypertensive genetic loci in Dss rats inflate BP effect upon BNP ablation, as Dss rats' exhibit higher mean BP compared to Dahl salt-resistant rats fed low salt diets. This is primarily caused by hypertensionogenic kidneys^{38, 39}, as illustrated in the paradigmatic transplant study of Dahl salt-resistant rats, with kidneys from Dss rat, resulting in hypertensive rats (i.e. hypertension following the kidney)³⁹.

From testing the salt-induced hypertensive sensitivity of *Nppb*^{-/-} rats, we have shown that both *Nppb*^{+/+} and *Nppb*^{-/-} rats are equally sensitive to high-salt-induced hypertension. Thus the mechanism of BP elevation induced by genetic deletion of BNP and salt-induced hypertension in Dss rats, are mutually exclusive.

Early alteration of cardiac function and structure in *Nppb*^{-/-} rats

Standard ECHO measurements demonstrated earlier LVH (i.e. three months) in *Nppb*^{-/-} rats, with impaired myocardial function as detected by strain and strain rate (Table 1 and 2), along with maintained ventricular emptying. Cardiac structure deterioration was predominantly similar to that in *Nppb*^{+/+} rats at six and nine months, showing an aging effect on the cardiac structure of the control rats. However, myocardial function was significantly and further impaired in the *Nppb*^{-/-} rats at nine months as indicated by speckle tracking data (i.e. global circumferential strain). The decreased strain and the strain rate data coincides with the demonstrated increase in myocardial fibrosis at nine month (Fig. 2), which may have contributed to the observed decrease of myocardial shortening and increased stiffness. The augmented fibrosis deposition could have ultimately caused the QT elongation documented at nine months (Figure 2D) in the *Nppb*^{-/-} rats.

The hypertensive prone phenotype of the Dss background of our model, may have blunted the differences observed between the *Nppb*^{-/-} and the *Nppb*^{+/+} rats, and in part explains the aging effects upon cardiac function and structure observed at ECHO examinations performed at six and nine months. Nevertheless, the more profound and earlier alterations observed resulting from BNP deletion were likely responsible for the increase in sudden death. The reduced number of surviving *Nppb*^{-/-} rats at six and at nine months could also have contributed to the lack of statistical difference. An alternative cause between the knock out phenotype of cardiac impairment, QT elongation, and sudden death, may be due to autonomic innervation. While not a direct measurement of autonomic innervation, levels of

Ngf expression within innervated tissues, such as the myocardium, roughly correspond to the innervation density⁴⁰. Ngf in knock out rats was decreased 1.26 fold from age-matched controls, suggesting the increased cardiac impairment in the *Nppb*^{-/-} rats was not due to innervated myocardial tissues. We further investigated heart rate variability (HRV), as an indirect assessment of sympathetic and parasympathetic activation. Previous studies, have shown that BNP, like other NPs, increases heart rate and electrical conduction by stimulating ionic currents in the sinoatrial node and atrial myocardium⁴¹. However, HRV was not different between groups at three and nine months. Together these data suggest that the autonomic nervous system may not play a critical role in the cardiac impairment of knock out rats.

Activation of cardiac remodeling pathways in the early phase of hypertension

Chronic BP elevation leads to cardiac remodeling, hypertrophy, increased fibrosis and stiffness, ultimately resulting in a decline of cardiac function. Studies have previously demonstrated that the NPs possess anti-hypertrophic and anti-fibrotic effects through binding receptor GC-A/Npr1. In addition, the anti-hypertrophic actions of the ANP/GC-A system are independent of BP⁴². GC-A/Npr1-null mice exhibit developmental cardiac hypertrophy⁴³, with anti-hypertensive treatments capable of normalizing BP elevation, but ineffective in reducing heart size⁴⁴. In contrast, we found no evidence of cardiac hypertrophy in one and two month-old *Nppb*^{-/-} rats. Similarly reported in BNP knockout mice²⁰, this suggests that physiological levels of BNP do not play a major role in developmental cardiac growth. In contrast, BNP-null rats demonstrated significant increases in LV mass and posterior wall thickness at three months, which was in concert with the beginning of elevated BP. Significant increases in cardiac stiffness and fibrosis were evident in *Nppb*^{-/-} at nine months, reinforcing the progressive nature of cardiac remodeling during hypertension. It is also notable that LV mass, along with activation of cardiac hypertrophy signaling pathway genes, preceded significant chronically elevated BP *Nppb*^{-/-}. This is in agreement with our previous observation in spontaneously hypertensive rats (SHRs) where cardiac BNP transduction prevented the development of cardiac remodeling, partly independently of BP reduction¹³. Here, at three months of age, BP elevation in knockout animals was marginal. Consistent with this, is the population-based study in adolescents and young adults demonstrating twofold higher prevalence of LVH among pre-hypertensive individuals⁴⁵. In addition, we observed marked up-regulation of cardiac fibrosis-associated genes, such as *Col1a1* and *Tgfβ*, prior to significant cardiac connective tissue deposition, in BNP-null rats at 3 months. Together with what we previously reported in SHRs and in humans with prehypertension^{6, 13, 14}, we suggest that relative BNP insufficiency leads to pre-activation of cardiac hypertrophic and profibrotic programs, prior to the development of true hypertension, contributing to a worsening of cardiac remodeling in later stages of life.

Renal protective effects of BNP

Nppb^{-/-} rats at nine months demonstrated higher levels of protein excretion and polyuria, with relatively unchanged creatinine clearance, as an estimate of glomerular filtration rate. This is in agreement with early studies assessing the accuracy of filtration markers such as creatinine, in chronic kidney disease. Authors inferred that patients would require a loss of greater than 50% in glomerular ultrafiltration in order for serum creatinine levels to increase

above the normal range⁴⁶. It is then possible that CKD patients preserve serum creatinine levels within the normal range, despite significantly reduced renal function⁴⁷. Knock out renal tissues further developed parenchymal remodeling, characterized by renal fibrosis, dilated proximal tubules, renal cast formation and increased glomerular injuries, more severely than age-matched controls. Specifically, we observed a tendency to express higher desmin and decreased podocin immunofluorescence, two markers of podocyte damage, in the *Nppb*^{-/-} rats. This was accompanied by micro-cysts formation predominantly at proximal tubules level, as indicated by positive LTA staining (Fig. 4E). These pathological changes are characteristic of hypertensive nephropathy and interestingly presented prior to an apparent reduction of renal function (i.e. decline in creatinine clearance). Progressive renal remodeling largely coincided with BP elevation, implying that chronic BP elevation is crucial to renal pathophysiology in *Nppb*^{-/-} rats. Nevertheless, the modest but significant increase in glomerular injuries as well as the activation of fibrosis associated genes at three months, prior to considerable hypertension, highlights the natural renoprotective effects of BNP that go beyond BP control. Like cardiac remodeling, it is conceivable that the BNP insufficiency may play a role in worsening of renal complications also in human hypertension.

Decline in the survival of the *Nppb*^{-/-} rats

A population-based study demonstrated that, compared with normotensive subjects, hypertensive subjects acquire shorter life expectancies and have fewer cardiovascular disease-free years⁴⁸. A hallmark of our BNP deficient rats was a shortened life expectancy. Most rats died prior to nine months, while no control rats died during the study period. Morbidity, and mortality onset was sudden, unexpected, with several rats found dead, or extremely weak (hunched and lethargic), a day following reasonable health. Since a clearly defined cause that precipitated lethal events remained unclear, we speculated that a number of factors contributed to the reduced survival. Since knock out rats at three and nine months frequently presented with substantially remodeled hearts, localized fibrosis, and notable thrombi, it is conceivable that cardiac arrest or embolism contributed to the sudden death. Additionally, we found elongated QT intervals, possibly secondary to the marked myocardial fibrosis, at nine months in *Nppb*^{-/-} rats, that could also explain the risk of sudden death. It should be noted that a prolonged QT interval is a major predictor of mortality in hypertensive patients^{49,50}. Last, a significantly deteriorated renal structure could also have contributed to the increased risk of death in these *Nppb*^{-/-} rats.

Reversal of BNP knockout phenotypes by AAV9 vector-mediated long-term BNP over-expression

An inherent problem associated with zinc-finger nuclease generated knockouts, is off-target deletions^{51, 52}. To confirm that the prevailing *Nppb*^{-/-} phenotypes observed, namely cardiac remodeling, hypertension, polyuria and reduced survival, were specific to the genetic ablation of BNP, and not due to an off target deletion, we conducted a pilot study where AAV vectors was used to deliver cardiac BNP in *Nppb*^{-/-} rats. Neonate littermates were randomly divided into reversal, or control groups. Reversal pups received AAV9 vectors constitutively expressing endogenous rat BNP, and were followed with littermate controls for nine months. Vector genomes were quantified at three and nine months as 2.7E7

and 2.13E5 vector genomes per ug of total cardiac DNA, respectively. When the codon-optimized rat BNP transgene expression levels were analyzed by real-time RT-PCR, expression levels at three months were significantly elevated (17.6 fold) in treated animals, while no significant elevation in transgene expression was noted at nine months, suggesting a gradual reduction in vector genomes in treated rat hearts. Vector mediated BNP over expression in *Nppb*^{-/-} protected against the cardiac hypertrophy and remodeling observed in untreated littermates (Supplemental Fig. S7A), significantly suppressed BP at three and six months compared to *Nppb*^{-/-} (Supplemental Fig. S7B), and though vector genomes, as well as vector mediated expression, had waned significantly over time, treated animals were protected against the polyuria experienced by *Nppb*^{-/-} littermate controls at nine months (Supplemental Fig. S7C). Six out of seven BNP-treated *Nppb*^{-/-} rats survived the study duration of nine months, with one rat dying due to anesthesia malfunction, verifying that BNP insufficiency was responsible for the key phenotypes; increased BP, cardiac remodeling, polyuria, and reduced survival found in *Nppb*^{-/-} rats.

A novel small animal model for human hypertension

Rodents provide excellent small animal models to study cardiorenal diseases. In particular, rats are favored for cardiovascular diseases over mice, due to their inherently similar cardiovascular physiology to humans. Their larger size facilitates higher resolution imaging, increased blood and tissue harvest potential, as well as surgical possibilities. Currently, various genetic and spontaneous rodent models are available to study hypertension. However, none faithfully recapitulate the development of human hypertension with BNP insufficiency. Rodent models with genetic *Nppa* or *GC-A* knockout exhibit congenital hypertrophy with systemic BP elevation. *Nppb*^{-/-} mice show focal cardiac fibrosis, however they do not present with progressive or naturally occurring BP elevation. In addition, BNP knock out mice do not develop secondary pathologies characteristic of human hypertension such as; polyuria, renal parenchymal remodeling or glomeruli pathologies, and altered myocardium. The *Nppb*^{-/-} rat exhibited adult-onset, progressive, systemic hypertension, with hypertension-associated cardiac and renal complications. Additionally, *Nppb*^{-/-} rats demonstrate LVH and sudden cardiovascular death without notable cardiac dysfunction, providing a unique platform to model metabolic and physiological properties of human hypertension. At six months, while the main cardiac functional parameters in the *Nppb*^{-/-} rats were not different from their age matched controls, LVM remained slightly higher. The lack of progressive worsening of LVH certainly represents a major difference in the evolution of hypertension between humans and our model. This difference is likely related to the background strain (i.e. hypertensive prone phenotype) of our *Nppb*^{-/-} rats (i.e. Dss) that it is characterized by a rapid transition from hypertrophied to dilated cardiomyopathy⁵³. Despite this inconsistency, this new model still allows for the assessment of interventions for hypertension, myocardial dysfunction (Table 2), and associated end-organ complications in a setting most closely mimicking human hypertension.

Perspectives

Our study furthers the role of BNP deficiency in developing hypertension and provides a unique and novel animal model of chronic hypertension with associated organ damage and reduced survival. Our study also warrants further interrogation on the applicability of

chronic BNP-based therapies for treating progressive hypertension and associated end-organ damages.

Supplementary Material

Refer to Web version on PubMed Central for supplementary material.

Acknowledgements

We would like to thank Dr. Kensuke Tsushima (University of Iowa) and Jim E. Tarara (Mayo Clinic) for helpful discussion and suggestions.

Funding Source: This work was supported by Mayo Foundation and the Center for Regenerative Medicine (to Y. Ikeda), NIH RO1 HL098502 (to A. Cataliotti and Y. Ikeda), Mayo PKD Center Pilot Study Award (to A. Cataliotti and Y. Ikeda, parent grant; NIDDK P30DK90728, PI: V. Torres), and grants NIH RO1 HL36634 and PO1 HL76611 (to J. C. Burnett).

References

1. Drazner MH. The progression of hypertensive heart disease. *Circulation*. 2011; 123:327–334. [PubMed: 21263005]
2. Rapsomaniki E, Timmis A, George J, Pujades-Rodriguez M, Shah AD, Denaxas S, White IR, Caulfield MJ, Deanfield JE, Smeeth L, Williams B, Hingorani A, Hemingway H. Blood pressure and incidence of twelve cardiovascular diseases: Lifetime risks, healthy life-years lost, and age-specific associations in 1.25 million people. *Lancet*. 2014; 383:1899–1911. [PubMed: 24881994]
3. Horvath K, Widimsky J Jr. Role of the heart as an endocrine organ. *Cor et vasa*. 1991; 33:441–450. [PubMed: 1842937]
4. Mukoyama M, Nakao K, Hosoda K, Suga S, Saito Y, Ogawa Y, Shirakami G, Jougasaki M, Obata K, Yasue H. Brain natriuretic peptide as a novel cardiac hormone in humans. Evidence for an exquisite dual natriuretic peptide system, atrial natriuretic peptide and brain natriuretic peptide. *J Clin Invest*. 1991; 87:1402–1412. [PubMed: 1849149]
5. Lang RE, Tholken H, Ganten D, Luft FC, Ruskoaho H, Unger T. Atrial natriuretic factor--a circulating hormone stimulated by volume loading. *Nature*. 1985; 314:264–266. [PubMed: 3157062]
6. Cataliotti A, Chen HH, Redfield MM, Burnett JC Jr. Natriuretic peptides as regulators of myocardial structure and function: Pathophysiologic and therapeutic implications. *Heart failure clinics*. 2006; 2:269–276. [PubMed: 17386896]
7. Fujisaki H, Ito H, Hirata Y, Tanaka M, Hata M, Lin M, Adachi S, Akimoto H, Marumo F, Hiroe M. Natriuretic peptides inhibit angiotensin ii-induced proliferation of rat cardiac fibroblasts by blocking endothelin-1 gene expression. *J Clin Invest*. 1995; 96:1059–1065. [PubMed: 7635942]
8. Fassett RG, Venuthurupalli SK, Gobe GC, Coombes JS, Cooper MA, Hoy WE. Biomarkers in chronic kidney disease: A review. *Kidney Int*. 2011; 80:806–821. [PubMed: 21697815]
9. Cataliotti A, Costello-Boerrigter LC, Chen HH, Textor SC, Burnett JC Jr. Sustained blood pressure-lowering actions of subcutaneous b-type natriuretic peptide (nesiritide) in a patient with uncontrolled hypertension. *Mayo Clin Proc*. 2012; 87:413–415. [PubMed: 22469356]
10. Ogawa Y, Itoh H, Tamura N, Suga S, Yoshimasa T, Uehira M, Matsuda S, Shiono S, Nishimoto H, Nakao K. Molecular cloning of the complementary DNA and gene that encode mouse brain natriuretic peptide and generation of transgenic mice that overexpress the brain natriuretic peptide gene. *J Clin Invest*. 1994; 93:1911–1921. [PubMed: 8182124]
11. Suganami T, Mukoyama M, Sugawara A, Mori K, Nagae T, Kasahara M, Yahata K, Makino H, Fujinaga Y, Ogawa Y, Tanaka I, Nakao K. Overexpression of brain natriuretic peptide in mice ameliorates immune-mediated renal injury. *J Am Soc Nephrol*. 2001; 12:2652–2663. [PubMed: 11729234]

12. Makino H, Mukoyama M, Mori K, Suganami T, Kasahara M, Yahata K, Nagae T, Yokoi H, Sawai K, Ogawa Y, Suga S, Yoshimasa Y, Sugawara A, Tanaka I, Nakao K. Transgenic overexpression of brain natriuretic peptide prevents the progression of diabetic nephropathy in mice. *Diabetologia*. 2006; 49:2514–2524. [PubMed: 16917760]
13. Tonne JM, Holditch SJ, Oehler EA, Schreiber CA, Ikeda Y, Cataliotti A. Cardiac bnp gene delivery prolongs survival in aged spontaneously hypertensive rats with overt hypertensive heart disease. *Aging*. 2014; 6:311–319. [PubMed: 24799459]
14. Cataliotti A, Tonne JM, Bellavia D, Martin FL, Oehler EA, Harders GE, Campbell JM, Peng KW, Russell SJ, Malatino LS, Burnett JC Jr. Ikeda Y. Long-term cardiac pro-b-type natriuretic peptide gene delivery prevents the development of hypertensive heart disease in spontaneously hypertensive rats. *Circulation*. 2011; 123:1297–1305. [PubMed: 21403100]
15. Arora P, Newton-Cheh C. Blood pressure and human genetic variation in the general population. *Current opinion in cardiology*. 2010; 25:229–237. [PubMed: 20224392]
16. Belluardo P, Cataliotti A, Bonaiuto L, Giuffrè E, Maugeri E, Noto P, Orlando G, Raspa G, Piazza B, Babuin L, Chen HH, Martin FL, McKie PM, Heublein DM, Burnett JC Jr. Malatino LS. Lack of activation of molecular forms of the bnp system in human grade I hypertension and relationship to cardiac hypertrophy. *American journal of physiology. Heart and circulatory physiology*. 2006; 291:H1529–1535. [PubMed: 16648193]
17. Macheret F, Boerrigter G, McKie P, Costello-Boerrigter L, Lahr B, Heublein D, Sandberg S, Ikeda Y, Cataliotti A, Bailey K, Rodeheffer R, Burnett JC Jr. Pro-b-type natriuretic peptide(1-108) circulates in the general community: Plasma determinants and detection of left ventricular dysfunction. *J Am Coll Cardiol*. 2011; 57:1386–1395. [PubMed: 21414536]
18. Macheret F, Heublein D, Costello-Boerrigter LC, Boerrigter G, McKie P, Bellavia D, Mangiafico S, Ikeda Y, Bailey K, Scott CG, Sandberg S, Chen HH, Malatino L, Redfield MM, Rodeheffer R, Burnett J Jr. Cataliotti A. Human hypertension is characterized by a lack of activation of the antihypertensive cardiac hormones anp and bnp. *J Am Coll Cardiol*. 2012; 60:1558–1565. [PubMed: 23058313]
19. Ogawa Y, Tamura N, Chusho H, Nakao K. Brain natriuretic peptide appears to act locally as an antifibrotic factor in the heart. *Can J Physiol Pharmacol*. 2001; 79:723–729. [PubMed: 11558681]
20. Tamura N, Ogawa Y, Chusho H, Nakamura K, Nakao K, Suda M, Kasahara M, Hashimoto R, Katsuura G, Mukoyama M, Itoh H, Saito Y, Tanaka I, Otani H, Katsuki M. Cardiac fibrosis in mice lacking brain natriuretic peptide. *Proc Natl Acad Sci U S A*. 2000; 97:4239–4244. [PubMed: 10737768]
21. Geurts AM, Cost GJ, Remy S, Cui X, Tesson L, Usal C, Menoret S, Jacob HJ, Anegon I, Buelow R. Generation of gene-specific mutated rats using zinc-finger nucleases. *Methods in molecular biology*. 2010; 597:211–225. [PubMed: 20013236]
22. Flister MJ, Tsaih SW, O'Meara CC, Endres B, Hoffman MJ, Geurts AM, Dwinell MR, Lazar J, Jacob HJ, Moreno C. Identifying multiple causative genes at a single gwas locus. *Genome research*. 2013; 23:1996–2002. [PubMed: 24006081]
23. Brody MJ, Hacker TA, Patel JR, Feng L, Sadoshima J, Tevosian SG, Balijepalli RC, Moss RL, Lee Y. Ablation of the cardiac-specific gene leucine-rich repeat containing 10 (Irrc10) results in dilated cardiomyopathy. *PloS one*. 2012; 7:e51621. [PubMed: 23236519]
24. Nasrallah R, Hebert RL. Prostacyclin signaling in the kidney: Implications for health and disease. *Am J Physiol Renal Physiol*. 2005; 289:F235–246. [PubMed: 16006589]
25. Paller MS, Manivel JC. Prostaglandins protect kidneys against ischemic and toxic injury by a cellular effect. *Kidney Int*. 1992; 42:1345–1354. [PubMed: 1474766]
26. Hama N, Itoh H, Shirakami G, Nakagawa O, Suga S, Ogawa Y, Masuda I, Nakanishi K, Yoshimasa T, Hashimoto Y, Yamaguchi M, Hori R, Yasue H, Nakao K. Rapid ventricular induction of brain natriuretic peptide gene expression in experimental acute myocardial infarction. *Circulation*. 1995; 92:1558–1564. [PubMed: 7664440]
27. Amin J, Carretero OA, Ito S. Mechanisms of action of atrial natriuretic factor and c-type natriuretic peptide. *Hypertension*. 1996; 27:684–687. [PubMed: 8613225]
28. Grantham JA, Burnett JC Jr. Bnp: Increasing importance in the pathophysiology and diagnosis of congestive heart failure. *Circulation*. 1997; 96:388–390. [PubMed: 9244198]

29. Bonow RO. New insights into the cardiac natriuretic peptides. *Circulation*. 1996; 93:1946–1950. [PubMed: 8640966]
30. Bruneau BG, de Bold AJ. Selective changes in natriuretic peptide and early response gene expression in isolated rat atria following stimulation by stretch or endothelin-1. *Cardiovascular research*. 1994; 28:1519–1525. [PubMed: 8001040]
31. Davidson NC, Naas AA, Hanson JK, Kennedy NS, Coutie WJ, Struthers AD. Comparison of atrial natriuretic peptide b-type natriuretic peptide, and n-terminal proatrial natriuretic peptide as indicators of left ventricular systolic dysfunction. *Am J Cardiol*. 1996; 77:828–831. [PubMed: 8623734]
32. Newton-Cheh C, Larson MG, Vasani RS, Levy D, Bloch KD, Surti A, Guiducci C, Kathiresan S, Benjamin EJ, Struck J, Morgenthaler NG, Bergmann A, Blankenberg S, Kee F, Nilsson P, Yin X, Peltonen L, Vartiainen E, Salomaa V, Hirschhorn JN, Melander O, Wang TJ. Association of common variants in nppa and nppb with circulating natriuretic peptides and blood pressure. *Nature genetics*. 2009; 41:348–353. [PubMed: 19219041]
33. Fraser TB, Turner SW, Mangos GJ, Ludbrook J, Whitworth JA. Comparison of telemetric and tail-cuff blood pressure monitoring in adrenocorticotropic hormone-treated rats. *Clin Exp Pharmacol Physiol*. 2001; 28:831–835. [PubMed: 11553024]
34. Kubota Y, Umegaki K, Kagota S, Tanaka N, Nakamura K, Kunitomo M, Shinozuka K. Evaluation of blood pressure measured by tail-cuff methods (without heating) in spontaneously hypertensive rats. *Biol Pharm Bull*. 2006; 29:1756–1758. [PubMed: 16880638]
35. Oliver PM, John SW, Purdy KE, Kim R, Maeda N, Goy MF, Smithies O. Natriuretic peptide receptor 1 expression influences blood pressures of mice in a dose-dependent manner. *Proc Natl Acad Sci U S A*. 1998; 95:2547–2551. [PubMed: 9482923]
36. Snajdar RM, Dene H, Rapp JP. Partial characterization of atrial natriuretic factor in the hearts of dahl salt-sensitive and salt-resistant rats. *Endocrinology*. 1987; 120:2512–2520. [PubMed: 2952493]
37. Dickey DM, Flora DR, Bryan PM, Xu X, Chen Y, Potter LR. Differential regulation of membrane guanylyl cyclases in congestive heart failure: Natriuretic peptide receptor (npr)-b, not npr-a, is the predominant natriuretic peptide receptor in the failing heart. *Endocrinology*. 2007; 148:3518–3522. [PubMed: 17412809]
38. Snajdar RM, Dene H, Rapp JP. Atrial natriuretic factor in inbred dahl salt-sensitive and salt-resistant rats. *Journal of hypertension. Supplement : official journal of the International Society of Hypertension*. 1986; 4:S343–347.
39. Dahl LK, Heine M, Thompson K. Genetic influence of the kidneys on blood pressure. Evidence from chronic renal homografts in rats with opposite predispositions to hypertension. *Circ Res*. 1974; 40:94–101. [PubMed: 4588315]
40. Shelton DL, Reichardt LF. Expression of the beta-nerve growth factor gene correlates with the density of sympathetic innervation in effector organs. *Proc Natl Acad Sci U S A*. 1984; 81:7951–7955. [PubMed: 6595669]
41. Springer J, Azer J, Hua R, Robbins C, Adamczyk A, McBoyle S, Bissell MB, Rose RA. The natriuretic peptides bnp and cnp increase heart rate and electrical conduction by stimulating ionic currents in the sinoatrial node and atrial myocardium following activation of guanylyl cyclase-linked natriuretic peptide receptors. *J Mol Cell Cardiol*. 2012; 52:1122–1134. [PubMed: 22326431]
42. Feng JA, Perry G, Mori T, Hayashi T, Oparil S, Chen YF. Pressure-independent enhancement of cardiac hypertrophy in atrial natriuretic peptide-deficient mice. *Clin Exp Pharmacol Physiol*. 2003; 30:343–349. [PubMed: 12859424]
43. Scott NJ, Ellmers LJ, Lainchbury JG, Maeda N, Smithies O, Richards AM, Cameron VA. Influence of natriuretic peptide receptor-1 on survival and cardiac hypertrophy during development. *Biochimica et biophysica acta*. 2009; 1792:1175–1184. [PubMed: 19782130]
44. Knowles JW, Esposito G, Mao L, Hagaman JR, Fox JE, Smithies O, Rockman HA, Maeda N. Pressure-independent enhancement of cardiac hypertrophy in natriuretic peptide receptor a-deficient mice. *J Clin Invest*. 2001; 107:975–984. [PubMed: 11306601]

45. Drukteinis JS, Roman MJ, Fabsitz RR, Lee ET, Best LG, Russell M, Devereux RB. Cardiac and systemic hemodynamic characteristics of hypertension and prehypertension in adolescents and young adults: The strong heart study. *Circulation*. 2007; 115:221–227. [PubMed: 17210838]
46. Shemesh O, Golbetz H, Kriss JP, Myers BD. Limitations of creatinine as a filtration marker in glomerulopathic patients. *Kidney Int*. 1985; 28:830–838. [PubMed: 2418254]
47. Bostom AG, Kronenberg F, Ritz E. Predictive performance of renal function equations for patients with chronic kidney disease and normal serum creatinine levels. *J Am Soc Nephrol*. 2002; 13:2140–2144. [PubMed: 12138147]
48. Franco OH, Peeters A, Bonneux L, de Laet C. Blood pressure in adulthood and life expectancy with cardiovascular disease in men and women: Life course analysis. *Hypertension*. 2005; 46:280–286. [PubMed: 15983235]
49. Oikarinen L, Nieminen MS, Viitasalo M, Toivonen L, Wachtell K, Papademetriou V, Jern S, Dahlof B, Devereux RB, Okin PM. Relation of qt interval and qt dispersion to echocardiographic left ventricular hypertrophy and geometric pattern in hypertensive patients. The life study. The losartan intervention for endpoint reduction. *J Hypertens*. 2001; 19:1883–1891. [PubMed: 11593111]
50. Oikarinen L, Nieminen MS, Viitasalo M, Toivonen L, Jern S, Dahlof B, Devereux RB, Okin PM. Qrs duration and qt interval predict mortality in hypertensive patients with left ventricular hypertrophy: The losartan intervention for endpoint reduction in hypertension study. *Hypertension*. 2004; 43:1029–1034. [PubMed: 15037560]
51. Gupta A, Meng X, Zhu LJ, Lawson ND, Wolfe SA. Zinc finger protein-dependent and -independent contributions to the in vivo off-target activity of zinc finger nucleases. *Nucleic Acids Res*. 2011; 39:381–392. [PubMed: 20843781]
52. Pattanayak V, Ramirez CL, Joung JK, Liu DR. Revealing off-target cleavage specificities of zinc-finger nucleases by in vitro selection. *Nat Methods*. 2011; 8:765–770. [PubMed: 21822273]
53. Inoko M, Kihara Y, Morii I, Fujiwara H, Sasayama S. Transition from compensatory hypertrophy to dilated, failing left ventricles in dahl salt-sensitive rats. *Am J Physiol*. 1994; 267:H2471–2482. [PubMed: 7810745]

Novelty and Significance

What's New?

- We've generated and characterized a new knock out rat; the Nppb^{-/-} Rat.
- Nppb^{-/-} rats exhibit adult-onset hypertension, with hypertension-associated cardiac and renal complications.
- Nppb^{-/-} rats demonstrate heart muscle thickening and sudden death without notable heart dysfunction.

What's Relevant?

- This new model provides a unique platform to better understand metabolic and physiological properties of human hypertension.
- The Nppb^{-/-} rat allows for the study of, and testing of, possible therapies for high blood pressure, heart dysfunction, and hypertension-associated complications, in a setting closely mimicking human hypertension.

Summary

- BNP knock out leads to progressive adult-onset hypertension, and hypertension associated organ damage, providing a new platform to better understand the development of, and test interventions against, hypertension.

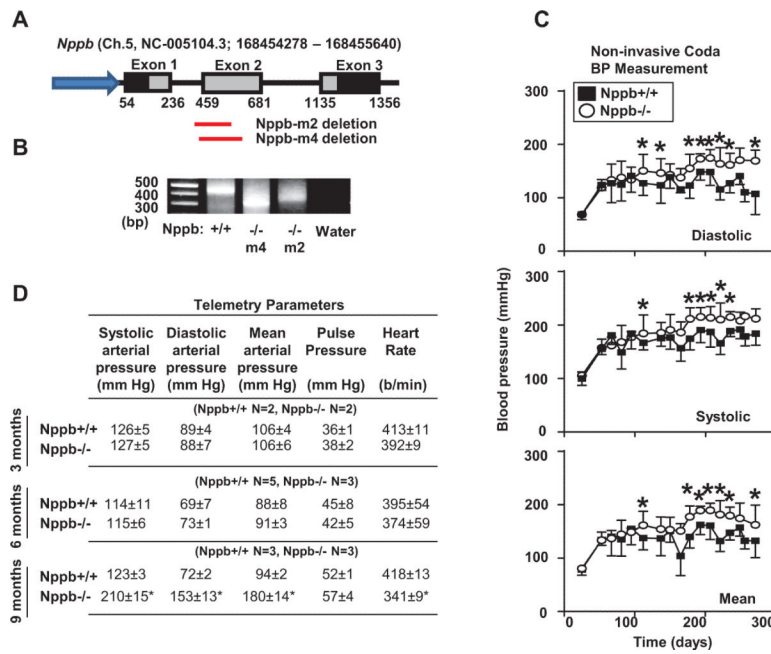
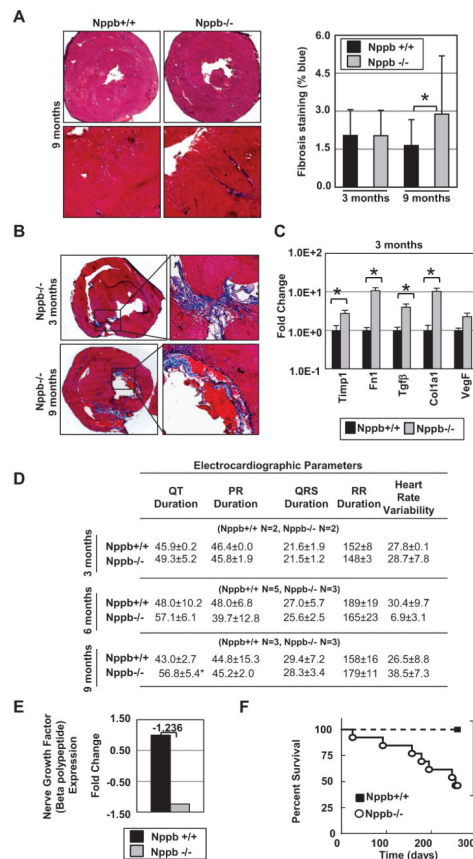


Figure 1. Physiological characterization of *Nppb*^{+/+} and *Nppb*^{-/-} rats. (A) Schematic organization of *Nppb* and ZFN generated targeted deletions in the M2 and M4 *Nppb*^{-/-} (B) PCR amplification of *Nppb* gene in *Nppb*^{+/+}, *Nppb*^{-/-} M2, and *Nppb*^{-/-} M4 strains, confirming 100 and 138bp deletions respectively. (C) Non-invasive blood pressure measurements; closed squares and open circles in *Nppb*^{+/+} (n=6) and *Nppb*^{-/-} (n=16) respectively. (D) Invasive blood pressure measurements at three, six and nine months of *Nppb*^{+/+} and *Nppb*^{-/-} rats. *, *p*<0.05; †, *p*<0.001, vs. *Nppb*^{+/+} rats.

**Figure 2.**

Cardiac phenotype of *Nppb*^{-/-} rats. (A) Quantification of Masson's trichrome blue staining at three (n=6, n=6) and nine months (n=6, n=6) *Nppb*^{+/+} and *Nppb*^{-/-} respectively with cardiac sections at nine months at 10x and 40x magnification. (B) Representative collagen, fibronectin deposition, and organized thrombi in young and aged *Nppb*^{-/-}. (C) RT-PCR quantification of *Timp1*, *Fn1*, *TGFβ*, *VegF* and *Col1a1* transcripts are shown, relative to 18S RNR. *Nppb*^{+/+} (n=6) and *Nppb*^{-/-} (n=6) at three months. Total RNAs (1μg) were analyzed, (D) ECG data from telemetry implants revealed a significantly elongated QT duration at nine months and similar heart rate variability (HRV) between control and *Nppb*^{-/-} rats, at three and nine months, (E) Nerve Growth Factor (NGF) expression, fold change, of cardiac tissues in *Nppb*^{+/+} (n=3) and *Nppb*^{-/-} (n=3) (F) Survival curve of *Nppb*^{+/+} (n=6) and *Nppb*^{-/-} (n=16) over nine months. Survival curves compared by log-rank (Mantel-Cox) test. *, *p*<0.05; †, *p*<0.001, vs. *Nppb*^{+/+} rats.

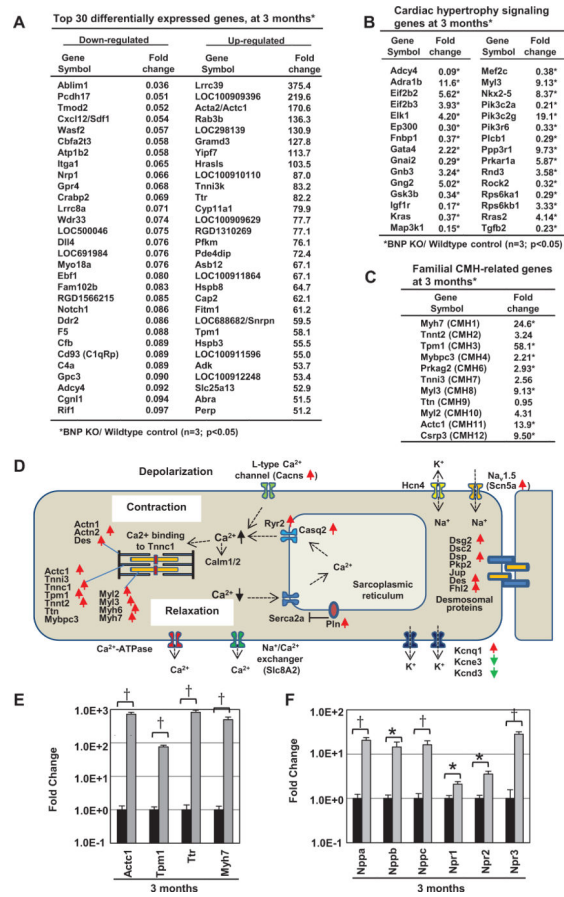


Figure 3. Gene expression profiling of cardiac tissues in *Nppb*^{+/+} (n=3) and *Nppb*^{-/-} (n=3). (A) Primary transcriptome analysis revealing cardiac repair, regeneration, contractility, and cAMP pathways differentially expressed in *Nppb*^{-/-} (B) Secondary analysis of the strongest differentially expressed pathways in *Nppb*^{-/-}, alongside canonical familial hypertrophic cardiomyopathy genes (C) demonstrating clear trends in enhanced contractility and increased Ca²⁺ influx. (D) Depiction of transcriptome analysis and modulated gene expression (red arrows, increased, green arrows, decreased) in the cardiomyocyte of *Nppb*^{-/-} rats. (E, F) Confirmed microarray expression of augmented Ttr, Actc1, Myh7, Tpm1, Nppa, Nppb, Nppc, Npr1, Npr2, and Npr3 transcripts in *Nppb*^{-/-} total cardiac RNA (1µg) relative to RNR. *Nppb*^{+/+} (n=6) and *Nppb*^{-/-} (n=6). *, p<05; †, p<001, vs. *Nppb*^{+/+} rats.

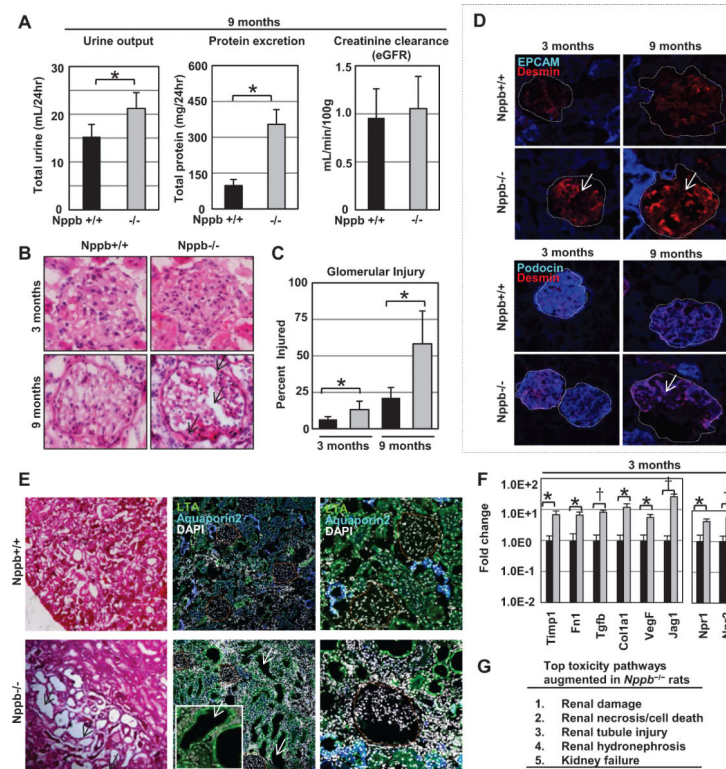


Figure 4. Renal phenotype of *Nppb*^{-/-} rats. (A) Quantification of 24hr urine excretion, proteinuria, and creatinine clearance in *Nppb*^{+/+} (n=6) and *Nppb*^{-/-} (n=5). (B) Representative hematoxylin and eosin stained sections, and (C) quantification of pathologic glomeruli in *Nppb*^{+/+} (n=6) and *Nppb*^{-/-} (n=6). (D) Representative microphotographs of immunofluorescent renal sections. Top; anti-EPCAM (blue), anti-Desmin (red) at three and nine months. Bottom; anti-Podocin (blue), anti-Desmin (red) at three and nine months. (E) Histology of Hematoxylin and Eosin stained renal tissues at nine months, revealing dilated tubules and renal casts (Left). Immunofluorescent renal sections identifying anti-LTA (green) positive staining of dilated tubules, antiaquaporin2 (blue) positive intact collecting ducts (middle, right), and nuclear staining with 4',6-diamidino-2-phenylindole (DAPI) (white). (F) Quantitative RT-PCR results of total RNA (1.0 μg) from renal tissues at 3 months of age, relative to 18s RNR, are shown, *Nppb*^{+/+} (n=6) and *Nppb*^{-/-} (n=6). (G) Gene expression profiling of renal tissues in *Nppb*^{+/+} (n=3) and *Nppb*^{-/-} (n=3). Primary transcriptome analysis revealing renal damage, renal necrosis / cell death, tubule injury, hydronephrosis, and kidney failure pathways differentially expressed in *Nppb*^{-/-}. *, $p < 0.05$; †, $p < 0.001$, vs. *Nppb*^{+/+} rats.

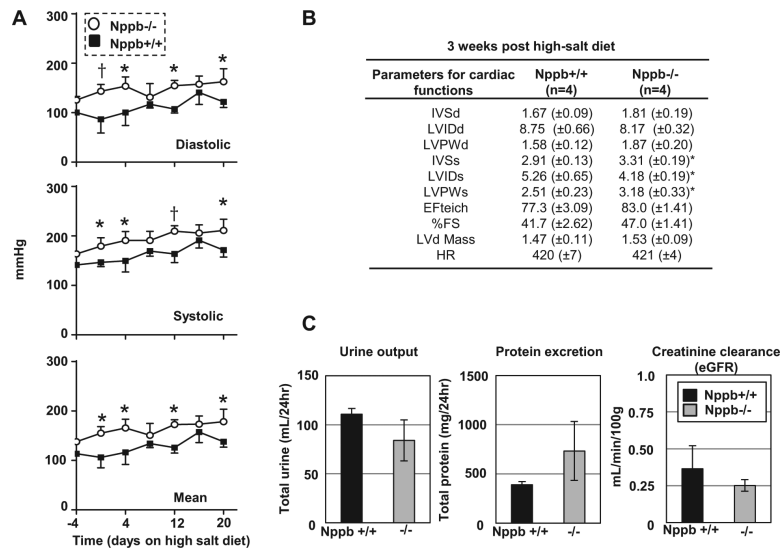


Figure 5. Characterizing salt-sensitivity of the Dss *Nppb*^{-/-}. (A) Non-invasive blood pressure measurements of *Nppb*^{+/+} (n=4) and *Nppb*^{-/-} (n=4) prior to, and during, three weeks on high-salt diet (B) Echocardiographic assessment of cardiac remodeling on high-salt diet three weeks post high-salt diet in *Nppb*^{+/+} (n=4) and *Nppb*^{-/-} (n=4). (C) 24 hour urine excretion, proteinuria, and creatinine clearance in *Nppb*^{+/+} (n=4) and *Nppb*^{-/-} (n=4) three weeks post high-salt diet. Blood pressure data calculated by two-wave ANOVA, Sidak's multiple comparisons test. *, *p*<05; †, *p*<001, vs. *Nppb*^{+/+} rats.

Table 1
Echocardiographic assessment of cardiac remodeling and function in *Nppb*^{-/-} and *Nppb*^{+/+}

Parameter:	1 month <i>Nppb</i> ^{+/+}	1 month <i>Nppb</i> ^{-/-}	2 months <i>Nppb</i> ^{+/+}	2 months <i>Nppb</i> ^{-/-}	3 months <i>Nppb</i> ^{+/+}	3 months <i>Nppb</i> ^{-/-}	6 months <i>Nppb</i> ^{+/+}	6 months <i>Nppb</i> ^{-/-}	9 months <i>Nppb</i> ^{+/+}	9 months <i>Nppb</i> ^{-/-}
Weight (g)	96 (±7)	79 (±21)	267 (±5)	253 (±30)	398 (±16)	378 (±20) [*]	438 (±21)	425 (±22)	462 (±19)	452 (±21)
IVSd (mm)	0.82 (±0.07)	0.81 (±0.10)	1.26 (±0.07)	1.21 (±0.12)	1.70 (±0.10)	2.01 (±0.08) [†]	1.84 (±0.09)	1.86 (±0.04)	2.41 (±0.14)	2.27 (±0.07)
LVIDd (mm)	5.70 (±0.36)	5.30 (±0.49)	8.11 (±0.35)	8.18 (±0.35)	7.53 (±0.07)	7.52 (±0.32)	8.48 (±0.08)	8.84 (±0.09) [*]	7.83 (±0.30)	8.88 (±0.22) [*]
LVPWd (mm)	0.90 (±0.05)	0.80 (±0.16)	1.28 (±0.17)	1.27 (±0.13)	1.72 (±0.06)	2.03 (±0.06) [†]	2.02 (±0.08)	1.81 (±0.09)	2.54 (±0.16)	1.85 (±0.14) [*]
IVSs (mm)	1.82 (±0.23)	1.95 (±0.33)	2.51 (±0.08)	2.53 (±0.24)	2.85 (±0.13)	3.19 (±0.20) [†]	3.26 (±0.08)	3.19 (±0.12)	3.81 (±0.16)	3.58 (±0.12)
LVIDs (mm)	3.09 (±0.61)	2.40 (±0.45)	4.21 (±0.41)	4.23 (±0.65)	3.98 (±0.16)	3.98 (±0.45)	4.51 (±0.13)	5.00 (±0.13) [*]	4.72 (±0.04)	5.46 (±0.37)
LVPWs (mm)	1.45 (±0.10)	1.48 (±0.19)	2.35 (±0.39)	2.34 (±0.56)	2.90 (±0.07)	3.29 (±0.19) [†]	3.29 (±0.13)	3.01 (±0.05)	3.77 (±0.11)	2.88 (±0.25) [*]
EFteich	83.2 (±7.2)	90.3 (±4.3)	85.8 (±2.8)	85.2 (±6.5)	83.3 (±2.0)	83.3 (±4.3)	85.0 (±1.0)	79.0 (±1.6) [*]	74.8 (±2.7)	74.2 (±3.4)
%FS	46.0 (±8.4)	54.9 (±6.9)	48.0 (±3.9)	48.3 (±8.1)	47.0 (±2.1)	47.3 (±4.1)	46.8 (±1.2)	43.4 (±1.5)	39.0 (±2.2)	38.8 (±2.6)
LVd Mass (g)	0.79 (±0.01)	0.75 (±0.05)	1.16 (±0.04)	1.15 (±0.02)	1.34 (±0.04)	1.53 (±0.08) [†]	1.64 (±0.02)	1.67 (±0.03) [*]	1.94 (±0.06)	1.84 (±0.03)
HR (bpm)	382 (±16)	344 (±43)	367 (±19)	390 (±8)	368 (±13)	382 (±45)	337 (±13)	351 (±8)	342 (±5)	347 (±4)

ECHO was performed on *Nppb*^{+/+} (n=5) and *Nppb*^{-/-} (n=7) at 1 month; on *Nppb*^{+/+} (n=5) and *Nppb*^{-/-} (n=6) at 2 months; on *Nppb*^{+/+} (n=6) and *Nppb*^{-/-} (n=10) at 3 months; on *Nppb*^{+/+} (n=5) and *Nppb*^{-/-} (n=5) at 6 months; *Nppb*^{+/+} (n=6) and *Nppb*^{-/-} (n=5) at 9 months.

Interventricular septum, diastole (IVSd), Left ventricular internal diameter, diastole (LVIDd), Left ventricular posterior wall, diastole (LVPWd), Interventricular septum, systole (IVSs), Left ventricular internal diameter, systole (LVIDs), Left ventricular posterior wall, systole (LVPWs), Ejection Fraction (EFteich), Percent fractional shortening (%FS), Left ventricular Mass, diastole (LVd Mass)

* p<0.05

[†] p<0.001, vs. *Nppb*^{+/+} rats.

Table 2

Speckle tracking assessment of myocardial strain

Age/Strain:	3 months Nppb+/+	3 months Nppb -/-	9 months Nppb+/+	9 months Nppb -/-
Circumferential Strain, <i>Global</i>	-18.7 (±10.0)	-16.4 (±10.0)	-15.2 (±6.7)	-11.7(±6.2) *
Circumferential Strain, <i>Systolic</i>	-14.9 (±11.4)	-9.8 (±15.2)	-12.84(±7.8)	-10.4(±6.0)
Circumferential Strain Rate, <i>Systolic</i>	2.2 (±2.8)	2.3 (±2.6)	1.5(±1.8)	1.6(±1.7)
Circumferential Strain Rate, <i>E-Diastolic</i>	-5.3 (±3.0)	-5.3 (±2.5)	-4.9(±1.9)	-4.1(±2.3)
Circumferential Strain Rate, <i>L-Diastolic</i>	6.6 (±3.0)	6.9 (±2.5)	4.7(±1.9)	4.8(±2.3)
Radial Strain, <i>Global</i>	5.5 (±2.9)	5.4 (±2.1)	4.7(±1.2)	4.2(±1.6)
Radial Strain, <i>Systolic</i>	51 (±12)	36 (±18) *	36(±24)	23(±5.6) *
Radial Strain Rate, <i>Systolic</i>	9.7 (±1.6)	8.4 (±2.1)	8.7(±3.2)	8.9(±5.4)
Radial Strain Rate, <i>E-Diastolic</i>	-13.0 (±2.9)	-9.1 (±4.4) *	-11.0(±3.8)	-8.4(±4.3) *
Radial Strain Rate, <i>L-Diastolic</i>	-8.6 (±2.9)	-10.0 (±2.7)	-11.0(±5.9)	-7.0(±1.9) *

At 3 months, ECHO was performed on *Nppb*^{+/+} (n=3) and *Nppb*^{-/-} (n=3); Speckle tracking assessment of myocardial strain was assessed by analyzing the parasternal short axis view of the left ventricle;

At 9 months, ECHO was performed on *Nppb*^{+/+} (n=5) and *Nppb*^{-/-} (n=6); Speckle tracking assessment of myocardial strain was evaluated by analyzing the parasternal short axis view of the left ventricle. E, early; L, late.

†, p <0.0001, vs. *Nppb*^{+/+} rats.

* p<0.05